*Particle Accelerators*, 1995, Vol. 50, pp. 1–17
Reprints available directly from the publisher
Photocopying permitted by license only



# SUMMARY OF THE WORKING GROUP ON IMPEDANCES

A.W. CHAO

*Stanford Linear Accelerator Center, Stanford University, Stanford, California 94309–0210, USA*

*(Received 12 December 1994; in final form 12 December 1994)*

The impedance working group concentrated on the LHC design during the workshop. We looked at the impedance contributions of liner, beam position monitors, shielded bellows, experimental chambers, superconducting cavities, recombination chambers, space charge, kickers, and the resistive wall. The group concluded that the impedance budgeting and the conceptual designs of the vacuum chamber components looked basically sound. It also noted, not surprisingly, that a large amount of studies are to be carried out further, and it ventured to give a partial list of these studies.

KEY WORDS: Collective effects, impedances, instabilities, linear accelerators: superconducting, synchrotrons: superconducting

## 1 INTRODUCTION

Collective instabilities in an accelerator are often caused by the electromagnetic interaction between the beam and its vacuum chamber environment. For relativistic beams, this interaction is most conveniently characterized by the longitudinal impedance $Z^{\parallel}$ and the transverse impedance $Z^{\perp}$, which are intrinsic characteristics of the vacuum chamber design of the accelerator. To understand quantitatively the collective behavior of the beam, it is critical to have a detailed and reliable knowledge of the impedances. The formation of an impedance working group in this workshop reflects the significance of this topic.

The impedance working group had two morning and two afternoon sessions available to discuss the various impedance issues of relevance to large hadron colliders. Due to a lack of time, we decided to concentrate on those issues specific to the Large Hadron Collider (LHC) presently being designed at CERN. This report is a summary of our discussions and deliberations. The topics covered below are arranged more or less in the chronological order as they were discussed by our group.

The participants in the Impedance Working Group were: F. Caspers, A.W. Chao, Y.H. Chin, K. Hirata, M.M. Karliner, S. Kurennoy, G. Lambertson, A.G. Mathewson, L. Palumbo, S. Petracca, A. Poncet, F. Ruggiero, T. Scholz, L. Vos, V.P. Yakovlev, G. Schröder.

## 2 THE LINER

The first topic of concern was the liner of the LHC design.[1] In the LHC, the proton beam produces a significant amount of synchrotron radiation. In the present design, a liner is inserted in the 2°K beam pipe to shield it from the radiation. Depending on the location relative to the nearest cooling pump, the temperature of the liner is between 5°K and 20°K.

The liner has slots cut along its length to allow proper vacuum pumping to reach the inside of the liner pipe. These slots, however, contribute to impedances. Since liners occupy a large fraction of the accelerator circumference, it is important that one knows these impedances in detail. With inputs from the present design and much discussions, the impedance group converged on a particular conceptual design as sketched in Figure 1.

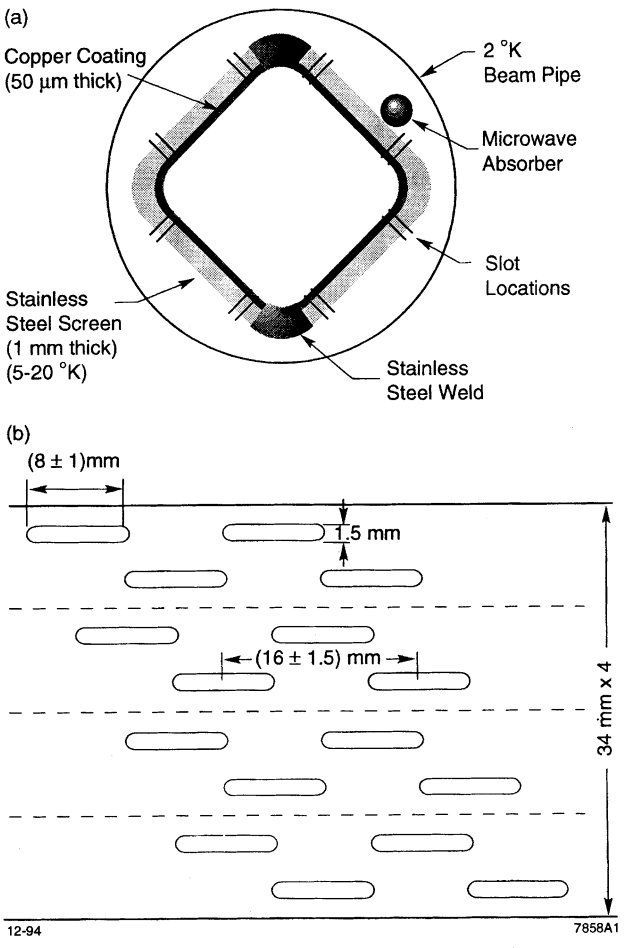


FIGURE 1: Sketch of the LHC liner.

Figure 1(a) is the cross-sectional view of the beam pipe and the liner. The beam pipe is round, while the liner is more or less square shaped. The liner is 1 mm thick and is made of a stainless steel material. Its inside (the side facing the beam) is coated with copper of 50 $\mu$m thickness. In the corners at the top and bottom of the liner, there are stainless steel welds, each a few millimeters wide, without copper coating. Attached to the outside surface of the liner (not touching the 2°K surface) is some arrangement of microwave absorbers.

The slots on the liner are arranged in a pattern shown in Figure 1(b), which shows the liner viewed as if cut along its length and expanded into a plane. The slots are arranged so that their long dimension is parallel to the liner axis. The slot width is 1.5 mm. The slot length is nominally 8 mm, but contains a random variation of 1 mm in rms. The slot ends are rounded. As shown in Figure 1(b), there are two rows of alternating slots on each of the four square surfaces of the liner, while the pattern is staggered from surface to surface. The longitudinal separation between adjacent slot centers is nominally 16 mm, but contains a random contribution of 1.5 mm in rms. There is no randomization on the transverse positions of the slots. Neither is there randomization in the slot width. The area covered by the slots is about 4.4% of the total surface area of the liner. This should be quite sufficient for vacuum pumping consideration.

The location of the welds at the top and bottom of the liner is approximately optimal from the impedance point of view as they are hidden in the corners. The transverse location of the slots at approximately 1/4 way off the center of the surface is nearly optimal as it more or less (a) minimizes the electromagnetic interactions with the beam, (b) minimizes the electromagnetic interactions among adjacent slots, and (c) maximizes the mechanical strength of the liner against a magnet quench.

## 3 LINER BROAD BAND IMPEDANCE

The broad band impedance of the liner slots can be predicted theoretically rather accurately. Little ambiguity exists in the theory.[2] More importantly, theory, computer simulation of the beam-slot interaction, and the bench measurements of the slot impedance all agree well as far as the broad band impedance is concerned.

A clever resonator technique was developed and used at CERN to measure the broad band impedance of the slots.[3] The experimental set-up is sketched in Figure 2.

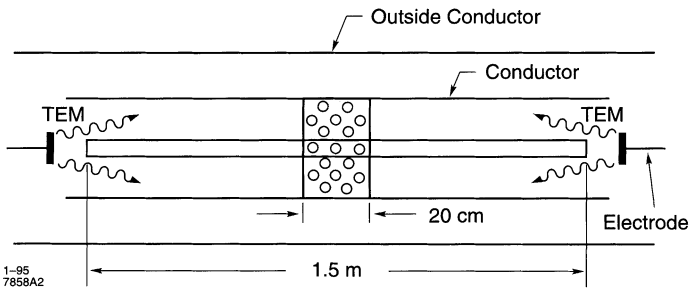


FIGURE 2: Resonator technique of measuring broad band impedances.

Two electrodes establish a standing TEM wave in a configuration consisting of a pipe and a conducting rod along the axis of the pipe. The TEM mode frequency is measured. A section of the pipe is then replaced by a short section (20 cm) with holes (or slots), and the mode frequency measured again. The shift of the mode frequency due to the holes then can be related to the imaginary part of the impedance of the holes. A measurement of the change in the $Q$-value of the mode gives the real part of the impedance. Since frequencies can be measured accurately, this gives accurate measurement of the imaginary part of the impedance. One disadvantage of this method is that the impedance can be measured only near the discrete TEM mode frequencies. It would be difficult to measure narrow band impedances this way.

Figure 3 shows some of the results obtained. The horizontal axis is the frequency. The vertical axis is the mode frequency shift. The solid straight line is the theoretical prediction of the frequency shift due to the purely inductive impedance of a 20 cm section filled with 4 mm holes. The theory predicts there are two contributions to the impedance, one electric in origin, and the other magnetic. These two contributions have opposite signs. After they partially cancel each other, the net effect gives the solid straight line. The resonator method, on the other hand, measures the electric and magnetic contributions with different weighting factors depending on details of the TEM wave pattern. In particular, alternating modes emphasize the electric and the magnetic contributions alternatingly. The net result is that the measured mode frequency shift is not expected to follow the straight line behavior. Instead, it should exhibit a zigzag behavior, as shown by the zigzag solid curve in Figure 3, which is the theoretically expected result of the measurements. Finally, the squares and circles are the measurement results. The agreement with theory is quite remarkable. This measurement offers a test of a subtle part of the theory — the part involving cancellation between the electric and magnetic contributions — and the theory has passed the test.

One concludes that the broad band impedance of the slots are not a serious technical issue. This part of the impedance can be calculated dependably, and for the LHC, it is calculated to give a value of $Z^{\parallel}/n = 0.03\ \Omega$, which is about 1/10 of the total impedance budget.[4]

The group discussed what remains to be done: (a) Extend the measurement to higher frequencies, perhaps up to 10 GHz. (b) Measure the real part of the impedance and compare with theory. (c) Measure the transverse impedance using two wires. (d) Replace holes by slots in the impedance section, and (e) vary the length of the impedance section.

## 4 LINER NARROW BAND IMPEDANCE

As mentioned, the broad band impedance of the liner is well predicted by theory. In particular, one expects the imaginary part of the broad band impedance to be inductive, and is proportional to frequency $\omega$. The real part of the impedance is expected to be proportional to $\omega^4$,[2] and is expected to be much smaller than the imaginary part up to a frequency whose corresponding wavelength is comparable to the slot width.

The broad band impedance, however, is not the only impedance contribution from the liner. Figure 4 gives a qualitative sketch of the liner impedance. In addition to the broad band impedance, there are narrow impedance peaks. The peak with the lowest frequency occurs at a wavelength comparable to the pipe size.

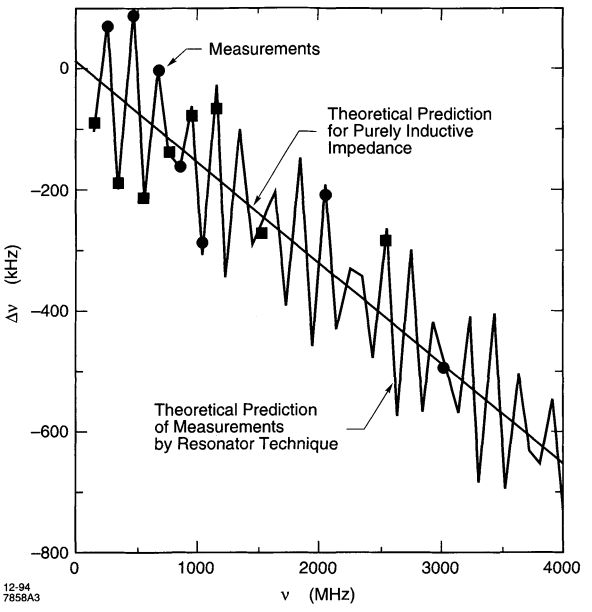


FIGURE 3: Results of impedance measurements of a liner section using the resonator technique.

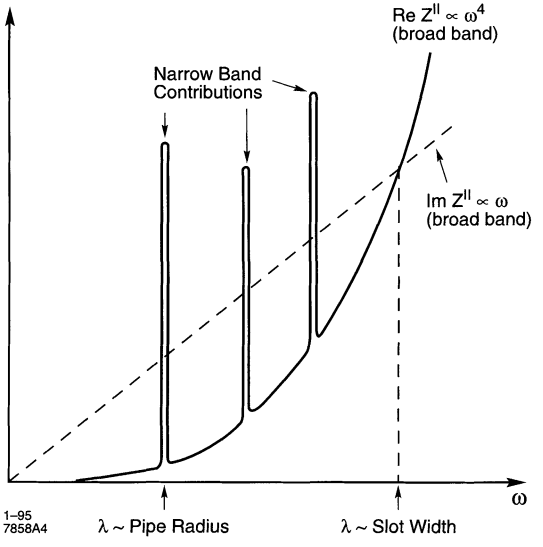


FIGURE 4: Sketch of the broad band and the narrow band impedance contributions of a liner with slots.

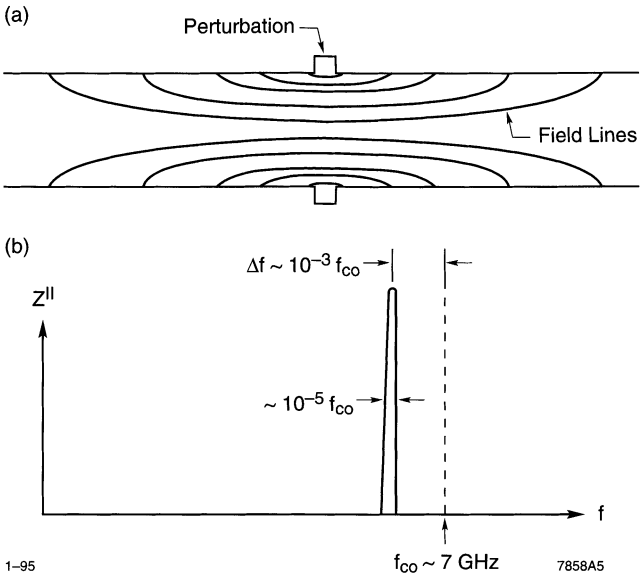


FIGURE 5: (a) Field pattern of a trapped mode. (b) Impedance of a trapped mode.

There are several possible sources of these narrow band contributions. These include (a) "trapped modes" which occur near cut-off frequencies, (b) periodic structure resonances which occur above cut-off frequencies, (c) possible resonances which occur when the wave resonates within one slot, i.e. when $\frac{n}{2} \times$ (wave length) = (slot length), where $n$ is an integer, and (d) possible resonances which involve two adjacent slots.[5]

Discussions of the group on these mechanisms are summarized below:

### *4.1 Trapped Modes*

Most of our discussions were on this mechanism of producing narrow band impedance peaks. According to theory,[2] when there is a small perturbation on an otherwise smooth vacuum chamber, there are "barely trapped" modes whose field lines look like Figure 5(a). The mode pattern extends for long distances from the small perturbation. The mode frequency is very close to, but slightly below, the cut-off frequency of the pipe. There is one trapped mode per each of the cut-off wave pattern of the pipe. For a slot, theory predicts that a trapped mode contributes to a narrow band impedance as sketched in Figure 5(b). For the LHC pipe geometry, the cut-off frequency occurs at about $f_{co} \sim 7$ GHz. The impedance peak occurs at a frequency about $\Delta f \sim 10^{-3} f_{co}$ below the cut-off frequency. The width of the peak is only about $10^{-5} f_{co}$ (i.e. $Q$-value is about $10^5$). It is also predicted that $\Delta f \propto A^2$, where $A$ is the area of the slot.

Adding the contributions from all the slots, one finds that a trapped mode has $Z^{\parallel} \approx 10\,\mathrm{M}\Omega$ at the peak, which corresponds to a value of $Z^{\parallel}/n \approx 300\ \Omega$.[2] This value of impedance would give rise to serious multi-bunch collective instabilities and has to be avoided.

At the time of the workshop, no such trapped modes have been observed experimentally. There was therefore the question whether these narrow band impedances were real. If these modes are found not to exist, one can of course ignore this part of narrow band impedance. If the theory proves to be correct, we must find a way to deal with these narrow band impedance. As mentioned before, the frequency of a trapped mode is located at $\Delta f \propto A^2$ below $f_{\mathrm{co}}$. By randomizing the slot area $A$ by 10%, therefore, these mode frequencies will acquire a spread of 20% $\times \Delta f$. Since $\Delta f$ is 100 times the natural spread of the trapped mode, this suppresses the effective $Q$ value of the trapped mode by a factor of 20. The value of $Z^{\parallel}/n$ is thus reduced to a much lower level of about 15 Ω. Hopefully, this would be sufficient to suppress the coupled-bunch instabilities.

Another way to introduce a spread in the mode frequency is to include a $10^{-3}$ variation in the vacuum pipe dimensions. This introduces a $10^{-3}$ variation in $f_{\mathrm{co}}$, which contributes to a similar spread in the trapped mode frequency.

The study of trapped modes is to be continued. (a) First thing to do is to find out experimentally whether trapped modes exist, and if they do, to find out their $Q$-values. (b) It is necessary to establish the narrow band impedance tolerance, and to see if $Z^{\parallel}/n =$ 15 Ω is indeed tolerable for coupled-bunch beam stability. (c) Regardless of the near term outcome of item (a), introduce a 10% random variation in the lengths of the slots.

### *4.2 Periodic Structure Resonances*

The periodic structure resonances can contribute to $Z^{\parallel}/n = 10\ \Omega$ with $Q = 10^5$.[2] This is probably not a serious problem, but since the cure is simple, it is suggested to randomize the positions of the slot centers by 10% to reduce the effective $Q$-value.

Note that trapped modes are dealt with by randomizing the slot lengths, while the periodic structure resonances are dealt with by randomizing the slot center positions.

### *4.3 Slot Length Resonances*

A resonant mode can be established along the length of a slot if the slot length $\ell$ is equal to an integral multiple of half wave length, i.e. when $\ell = n\frac{\lambda}{2}$. This is most likely not a problem because fields are probably not trapped for long by the slot. There is also experimental evidence that the $Q$-value of these modes are only of the order of 10–20 or so.[6] Furthermore, these modes may not couple to the beam easily.

### *4.4 Double Slot Modes*

The double-slot mechanism involves field lines threading through and looping around two adjacent slots. Both theoretical and experimental studies are lacking on this effect. It is believed that this mechanism is most likely a weak one. The alternating and staggered slot arrangement [see Figure 1(b)] should minimize this effect.

## 5 SLOT SHAPE

To minimize the broad band impedance of the slots, the slot ends should have an "aerodynamic" shape. The more aerodynamic the ends are shaped, the smaller the

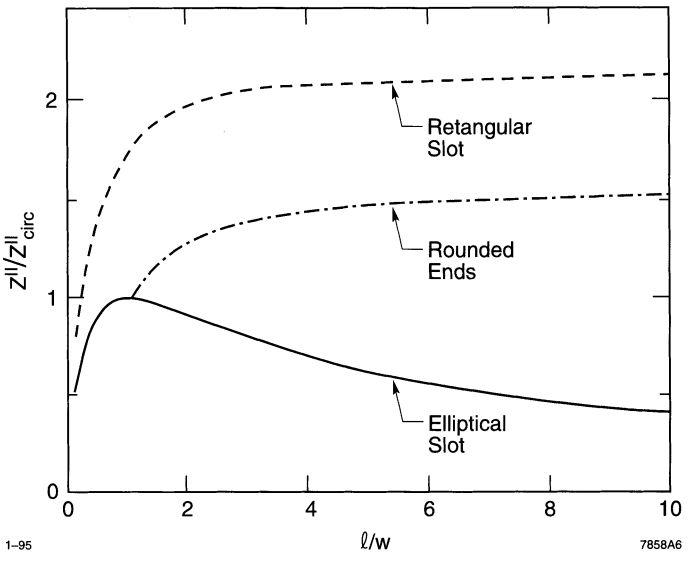


FIGURE 6: Broad band impedance $Z^{\parallel}$ of a slot, normalized by the impedance $Z^{\parallel}_{circ}$ of a circular hole versus of ratio of the slot length $\ell$ to the slot width $w$. Three cases shown are for a rectangular slot, a slot with rounded ends, and an elliptical slot.

impedance is. Compare the cases of the rectangular ends, the rounded ends, and the elliptical shaped slots for example. If the total length $\ell$ and the total width $w$ (measured at the middle of the slot) of the slot is fixed, and only the slot shaped is varied, the ratio of the three broad band impedances is about 3:2:1 when $\ell/w = 4$. Figure 6 gives these three impedances (normalized to the broad band impedance of a circular hole of diameter $w$) as functions of $\ell/w$.

The elliptical case has the smallest impedance. However, as mentioned before, the broad band impedance is not considered a critical problem, and since elliptical slots are more difficult to manufacture, the rounded ends are in the present design of the LHC slots.

## 6 MICROWAVE PENETRATION THROUGH THE SLOTS

Figure 7(a) shows the beam traveling down the beam pipe with long slots cut along the length of the pipe. The image currents carried by the beam passes by the slots aerodynamically as shown in Figure 7(b). Very little wake fields are generated either inside the liner or outside the beam pipe into the coaxial region between the liner and the beam pipe. However, if there are spurious microwaves with the "wrong" polarity as sketched in Figures 7(c) and 7(d) in the liner, these microwaves will easily penetrate the slots into the coaxial region. Long slots are designed to minimize the impedance, i.e. the response to fields and image currents carried by the beam, but are the worst one can do in terms of these "wrong" microwaves.

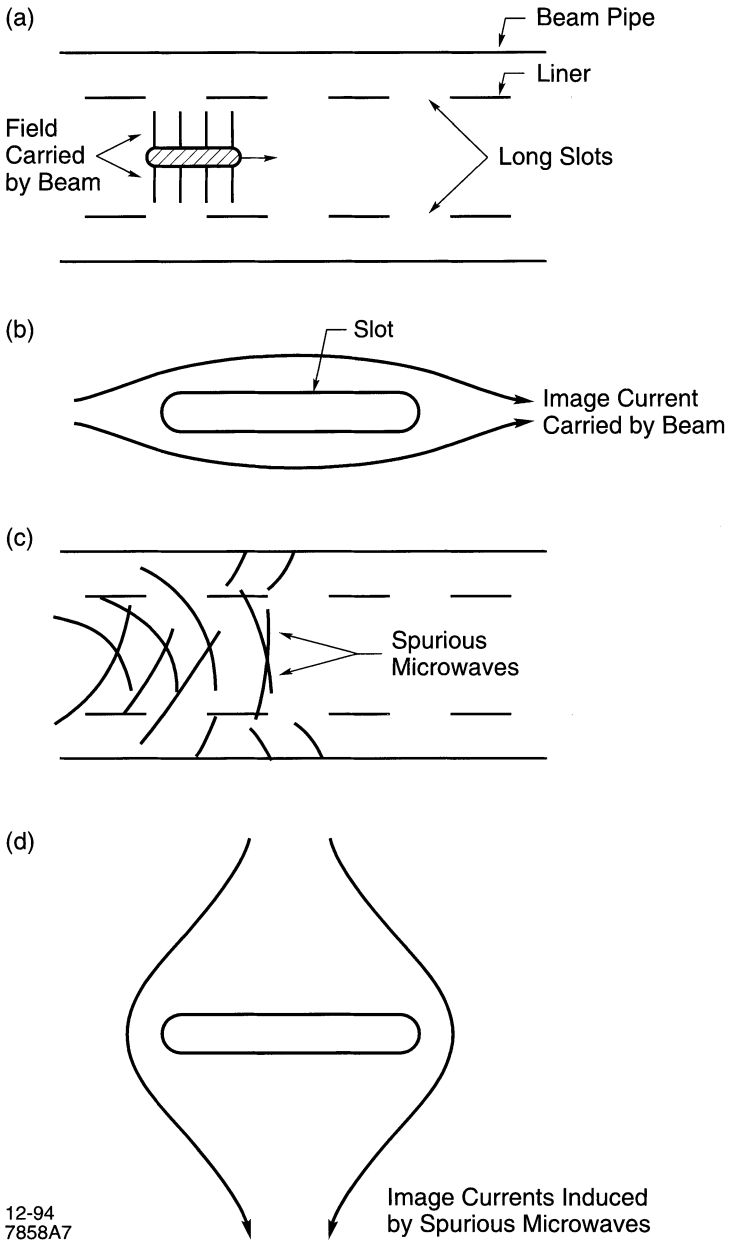


FIGURE 7: (a) Long slots shield the fields carried by the beam from entering the coaxial region. (b) Image currents carried by the beam passes the slot aerodynamically. (c) Spurious microwaves may have a polarity that allow easy penetration into the coaxial region. (d) Image currents induced by the spurious microwave.

Since the outer wall of the coaxial region is maintained at 2°K, the depositing of microwave energies there is of concern, even though only a small fraction of the fields in the liner pipe is of this "wrong" type. These wrong microwaves can be generated by the beam-induced wake fields after bouncing off some corners in the beam pipe. Their strength may depend on the beam closed orbit offset. It may also depend on whether the beam is undergoing some microwave instability such as turbulent bunch lengthening. It is noted also that this microwave penetration can occur in a rather localized manner (such as near the rf cavities). A similar consideration of this effect has been taken into account in the B-factory design at SLAC.[7]

To deal with this potential problem, it is suggested to include some microwave absorbers in the coaxial region in the LHC design. The absorber is to be attached to the liner, not to the outer 2°K wall. These absorbers also serve another function, namely, they disrupt the propagation of any possible TEM waves in the coaxial region. Such TEM waves may have resonant effect back onto the beam as both the waves and the beam travel with the speed of light. By disrupting the waves, the synchronism between the TEM wave and the beam is presumably destroyed.

Things to do include: (a) Estimate how much microwave power with the wrong polarity is contained in the beam and in the liner pipe. (b) Estimate how much (and what material) microwave absorber is needed per meter.

## 7 IMPEDANCE CATALOGUE AND BUDGET

Various vacuum chamber components have been evaluated for their impedance contributions. Their longitudinal broad band impedance contributions are listed in Table 1 below:[4]

TABLE 1: LHC Impedance Catalogue and Budget

| Component | $Z/n$ ($\Omega$) |
|---|---|
| Shielded bellows | 0.082 |
| Stripline monitors | 0.127 |
| Monitor tanks | 0.04 |
| Pumping slots | 0.037 |
| Kickers (injection & dump) | $< 0.1$ ? |
| Superconducting & damping cavities | 0.01 |
| Experimental chambers | 0.01 |
| Beam collimators | |
| Injection septum | |
| Recombination chambers | |
| Gate valves | |
| Electrostatic transverse dampers | |
| Low-$\beta$ quadrupoles | |
| Aperture transitions (warm-to-cold) | |
| Aperture transitions (square-to-round) | |
| Resistive wall | |

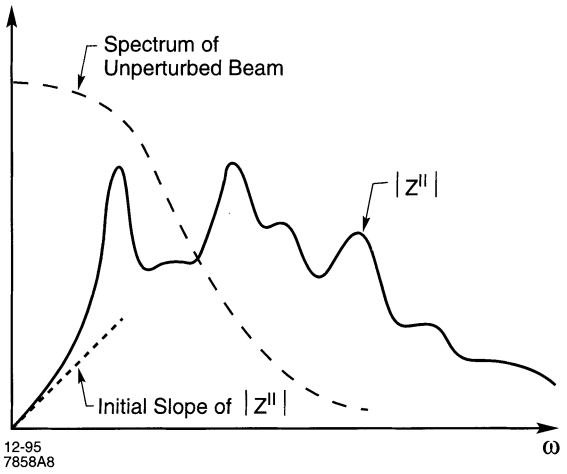


FIGURE 8: Sketch of a typical broad band impedance and spectrum of the unperturbed beam distribution.

The most important impedance offenders are the beam-position monitors, the shielded bellows, and possibly the kickers. Many of the lesser contributors are yet to be evaluated. Not all items in the table were discussed by the group, but the important ones were.

Before detailing the discussions of the group, there are a few general remarks concerning the impedance cataloguing and budgeting. The impedance budget has been done in terms of the quantity $Z^{\parallel}/n$. This is one convenient and appropriate way to characterize the broad band impedances. However, it is also important to recognize that $Z^{\parallel}/n$ alone is not sufficient to cover all the important beam dynamics.[8] For beam dynamics reasons, one needs more detailed information than the single quantity $Z^{\parallel}/n$. Figure 8 is a sketch of a broad band impedance and a spectrum of the unperturbed beam. In increasing order of details, the impedance information is contained in the following quantities:

(a) A crude estimate of $Z^{\parallel}/n$ can be obtained from the initial slope of the impedance (dotted line in Figure 8). This $Z^{\parallel}/n$ determined by the initial slope is useful only at very low frequencies, and is most likely insufficient for beam dynamics studies as the beam spectrum (dashed curve in Figure 8) typically extends to higher frequencies.

(b) One may use the effective impedance $(Z^{\parallel}/n)_{\text{eff}}$ which is the value of $Z^{\parallel}/n$ integrated over frequency weighted by the beam spectrum. (Another quantity in this same category is the loss factor $k_{\text{loss}}$.) This is a better quantity to characterize the beam dynamics than the $Z^{\parallel}/n$ of the initial slope, but it is sometimes still insufficient to address detailed beam dynamics.

(c) Further details are needed in studies such as the potential well distortion effect. The beam shape may be distorted due to wake fields, and the distortion may have important structures shorter than the unperturbed bunch length. In that case, one needs to know the impedance at higher frequencies than that contained in $(Z^{\parallel}/n)_{\text{eff}}$.

(d) Microwave instabilities often involve high order modes whose frequncies are several times the unperturbed bunch spectrum. Again, $(Z^{\parallel}/n)_{\text{eff}}$ is insufficient to cover these effects.

Due to these reasons, it is suggested that the impedance catalogue be extended to beyond what is contained in Table 1, perhaps to include the impedances as functions of frequencies up to 10 GHz. One should also calculate the corresponding wake functions down to distances much shorter than the unperturbed bunch length.

## 8 BEAM POSITION MONITORS

In Table 1, the BPM impedance is estimated in two parts: one from the striplines, the other from the monitor tank. The contributions to $Z^{\parallel}/n$ are estimated to be 0.127 Ω and 0.04 Ω respectively. Each BPM is assumed to have 4 striplines. Figure 9 is a sketch of the present BPM design.[9]

Beam position monitors are the largest source of broad band impedance for the LHC. As such it is worth asking whether there are ways to reduce or to eliminate BPMs as an impedance source. One idea is to replace BPMs by striplines *outside* of the liner screen, perhaps right behind the slots. These striplines do not contribute much to the impedance as seen by the beam. Nevertheless, a small field leakage through the slots should be sufficient to provide signals of the beam position in the beam pipe.[10] There is however a caveat: beam position measurement accuracy will be limited by the magnet alignment accuracy, which may not be sufficient.

Another idea is to keep the BPMs more or less as is, but introduce tapered "fins" between the BPM striplines. The purpose of these tapered fins is to conduct the image wall currents, thus significantly reducing the impedance.[11]

The monitor tank is a cavity structure, which may allow trapped modes. It is suggested that calculations and measurements be performed on these tanks to examine this issue. It is also suggested to examine if there are gains to be made by reducing the tank size (particularly the 4 mm tank depth shown in Figure 9. This would be a possibility if synchrotron radiation on the BPM striplines is not as serious a problem as previously envisioned.[9]

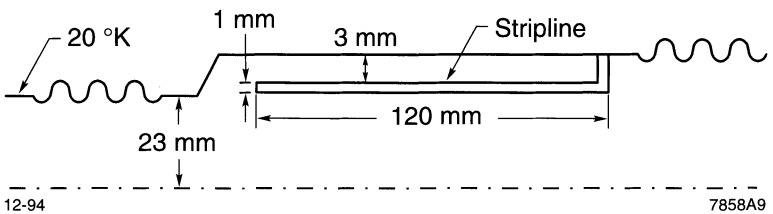


FIGURE 9: Sketch of the LHC BPM as seen by the beam. In Figures 9 to 11, only half the geometries are shown, assuming axial symmetry.

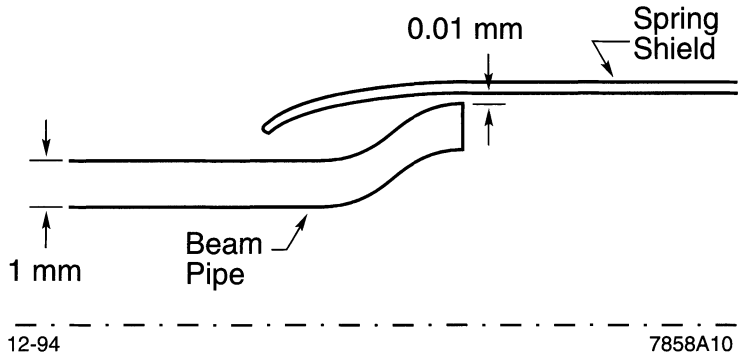


FIGURE 10: Sketch of the shielded bellows as seen by the beam.

## 9 SHIELDED BELLOWS

A sketch of a shielded bellows is given in Figure 10 (Only the pipe discontinuities as seen by the beam are shown). The bellows are the second largest impedance source in the present LHC design. Shielding of the bellows is necessary to reduce the broad band impedance down to the value listed in Table 1. The shielding is provided by introducing spring fingers which maintain a sliding contact with the beam pipe. The estimated contribution of 0.082 $\Omega$ to $Z^{\parallel}/n$ is obtained by scaling to the similar bellows design of the (by-now extinct) Superconducting Super Collider.

There are two impedance effects to be considered. The broad band $Z^{\parallel}/n$ comes mainly from the 1 mm discontinuity in the design (see Figure 10). In addition, there is an estimated 1 kW/ring parasitic heating in the bellows. This heating comes mainly from the assumed 0.01 mm gap between the beam pipe and the spring shield. In case the spring shield makes good contact with the beam pipe, as the design is meant to accomplish, this parasitic heating will be much reduced.

It is suggested, as the next iteration of the bellows impedance estimation, that an LHC-specific calculation be performed with the proper design geometry. It is also suggested that failure modes be carefully analyzed. For example, if one of the spring fingers breaks, (a) what happens to the broad band impedance? (b) what is the effect on the parasitic heating? (c) are there going to be accidental weldings due to sparks? It is likely that the effect on the broad band impedance is small, but the effect on the parasitic heating may not be negligible.

## 10 EXPERIMENTAL CHAMBERS

The vacuum chamber structure near the interaction points is made to incorporate the detector requirements. The present design is sketched in Figure 11.[4] The $Z^{\parallel}/n$ is estimated to be

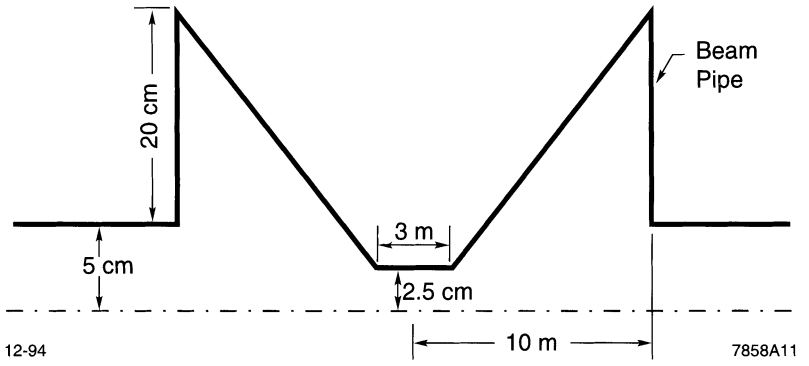


FIGURE 11: Experimental chamber as seen by the beam. Note the longitudinal and radial scales are different.

0.003 Ω, which is rather small. However, in addition to the broad band impedance, this cavity-like structure can be rich in trapped modes with high $Q$-values. It is suggested that these possible trapped modes be evaluated. In the calculation of the wake fields of the experimental chambers, it is suggested that, in order to obtain sufficiently accurate results, one applies a fine mesh (at least in the radial direction).[12]

## 11 SUPERCONDUCTING CAVITIES

A sketch of the LHC superconducting cavity structure is shown in Figure 12. The two ends of the cavity structure are tapered in order to minimize the broad band impedance. The taper angle is 6.7°. Cavity fundamental and higher order modes have been calculated and been used in the calculation of coupled-bunch instability growth rates.[4]

The KEK superconducting cavity design was found to have a rather substantial loss factor of 2.5 V/pC.[13] The KEK design has a much larger tapering angle (18°) and a shorter bunch length than the LHC case, so the LHC loss factor is expected to be much smaller. But it is suggested that a careful evaluation be made to see if there is excessive heating of the rf cavities in the LHC case.

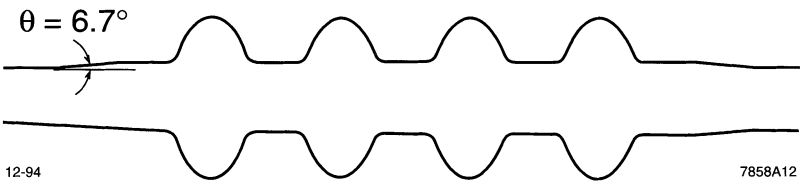


FIGURE 12: Superconducting cavity structure as seen by the beam.

## 12 RECOMBINATION CHAMBERS

A recombination chamber is where two vacuum beam pipes (for the two beams) merge into one. This occurs on each side of the interaction points. There is not yet a conceptual engineering design of the recombination chamber for the LHC. Two issues need to be studied.[14] One is the expected $Z^{\parallel}/n$ budget. The other is to estimate how much parasitic heating is induced as the fields carried by one beam is scraped off when the beam is deflected into one of the two channels. This parasitic heating may not be a problem because this energy loss, unlike the parasitic heating of the BPM shield gaps, occurs in a room-temperature region.

## 13 SPACE CHARGE

The direct space charge tune shift is found to be[4] $\Delta Q = 0.0012$ at 450 GeV and beam intensity of $1 \times 10^{11}$ particles per bunch. The Laslett tune shift is found to be 0.017 under the same conditions. The space charge is not believed to be a serious problem in the LHC main rings. However, it is noted that the Laslett coefficients acquire a tensor nature when one considers the complications of an elliptical beam in a squarish pipe.[15] It is also pointed out[4] that the transient behaviour shortly after injection of a beam batch would be a complex phenomenon and needs to be investigated.

## 14 KICKERS

There seem to be a variety of kicker designs adopted in the various accelerators. The presently envisioned kicker design for RHIC[16] for example looks very different from the existing kicker design at DESY.[17] This is further complicated by the fact that there are several technical considerations for a kicker to fulfill. Given this situation, the group decided to create a conceptual design of their own for an "ideal" kicker, which includes all the bells and whistles to deal with each of the technical considerations identified. This "ideal" design is sketched in Figure 13. It has the following features:

(a) Its ferrite has an H-shaped (instead of C-shaped) configuration. This symmetry reduces the $\dot{B}$-induced voltage along the beam path, which may lead to breakdown somewhere either inside or outside the kicker assembly.

(b) There is a thin (a few microns thickness) of titanium coating on the inside of the ceramic beam pipe. This is to reduce the high frequency impedance seen by the beam, to shield the beam fields from leaking into the magnets, and to conduct away the static charge that might have accumulated.

(c) There are 2 copper strips located at the top and bottom of the beam pipe. These are to reduce the low frequency impedance. The strips are preferably inside the ceramic chamber because it helps against breakdowns inside. It also aids the titanium coating in reducing the high frequency impedance.

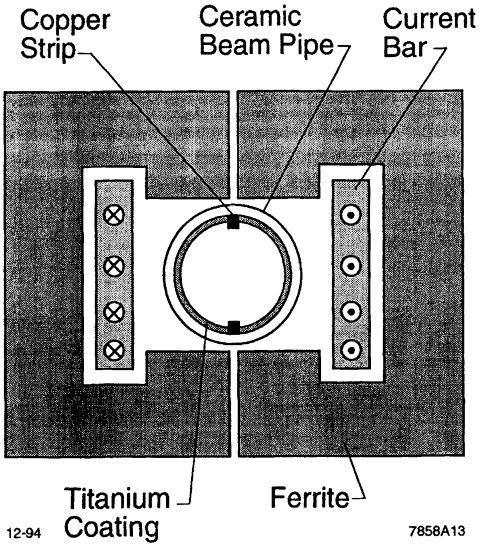


FIGURE 13: An "ideal" kicker design.

An LHC kicker design was presented in the workshop,[18] and it turned out very close to the "ideal" design. The only deviation is that the function of the copper strips are to be assumed by two copper plates between the ferrites on the outside of the ceramic chamber, but this is regarded as a minor deviation.

The question that remains is then whether all bells and whistles of the "ideal" design are actually needed for the LHC. In particular, measurements performed at RHIC seem to indicate that, without a titanium coating, the two copper strips on the outside of the ceramic chamber already reduce the broad band impedance by a factor of 3.[16] One may also ask if it suffices to have a titanium coating without the copper strips.

Further studies include: (a) How thick does the titanium coating have to be? Are there ways to coat titanium on ceramic thicker than a few microns? (b) If no copper strips are included, what are the effects of the covering tank in terms of low frequency trapped modes?

## 15 RESISTIVE WALL

The copper coating on the inside of the liner has to be thick enough to keep the resistive wall coupled-bunch instability within the control of the feedback systems, and to keep the parasitic heating to a tolerable level. It also must be thin enough so that the eddy-current induced stress force does not crush the liner when the dipole magnet quenches. The quench force consideration dictates that the copper coating must be thinner than 100 $\mu$m, and preferably thinner than 50 $\mu$m.[19] The liner temperature is designed to be between 5°K and 20°K.[20]

The coupled-bunch instability growth rate depends on the specification on how much room between the betatron tunes to integers needs to be reserved for beam operations. In order not to overly restrict the choice of the betatron tunes, one must consider the instability down to a sufficiently low frequency.[21] If one takes a frequency of 3 KHz (corresponding to a distance $> 0.3$ of the betatron tunes from integers), and assume a copper thickness of 50 $\mu$m, the growth times are estimated to be 28 ms at 450 GeV, and 200 ms at 7.7 TeV.[22] The parasitic heating is estimated to be 0.2 W/m at 450 GeV and 0.3 W/m at 7.7 TeV. In comparison, if the copper coating is 20 $\mu$m thick, the growth rate at 450 GeV would be 11 ms.[4] The present design with 50 $\mu$m copper thickness seems adequate.

The welds at the top and bottom of the liner must not occupy too much surface area because they are not copper coated. It is estimated that if they occupy 50% of the liner surface area, the parasitic heating will reach 2 W/m level, which is not acceptable.[22] The present design with only a few percent of area covered by the welds is fine.

The warm regions along the accelerator circumference also contribute to the resistive wall impedance. Since the skin depth in the warm region is much larger than in the cold region, the beam pipe in the warm regions is to be made of copper. Assuming the pipe is 2 mm thick and has a radius of 5 cm, and assuming the warm regions occupy a total of 10% of the machine circumference, it is estimated that the growth time decreases from 28 to 21 ms at 450 GeV.[4]

REFERENCES

1. The LHC Study Group, Design Study of the Large Hadron Collider (LHC), CERN 91–03, 1991.
2. S. Kurennoy, proceedings of this workshop, and references quoted therein.
3. T. Scholz, proceedings of this workshop.
4. F. Ruggiero, proceedings of this workshop.
5. G. Lambertson, communication, this workshop.
6. F. Caspers, communication, this workshop.
7. A. Chao, E. Daly, S. Heifets, C.-K. Ng, M. Nordby, W. Stoeffl, G. Stupakov, T. Weiland, 'Study of the slot impedance for the PEP-II High Energy Ring,' 1994.
8. L. Palumbo, communication, this workshop.
9. L. Vos, communication, this workshop.
10. F. Caspers, communication, this workshop.
11. F. Caspers, G. Lambertson, communication, this workshop.
12. Y.H. Chin, communication, this workshop.
13. Y.H. Chin, proceedings of this workshop.
14. K. Hirata, communication, this workshop.
15. S. Petracca, proceedings of this workshop.
16. S. Peggs, communication, this workshop.
17. F. Willeke, communication, this workshop.
18. G. Schröder, communication, this workshop.
19. A.G. Mathewson, communication, this workshop.
20. A. Poncet, communication, this workshop.
21. J. Gareyte, communication, this workshop.
22. M.M. Karliner, N.V. Mityanina, B.Z. Persov, V.P. Yakovlev, proceedings of this workshop.